

# Experimental Study on Two Storied Traditional Wooden Houses in Japan

**Y. Hayashi, A. Nakagawa & N. Takiyama**  
*Kyoto University, Japan*

**S. Hirosue**  
*Obayashi Corporation, Japan*



## SUMMARY:

We have conducted static loading tests of plane frame of a two-storied traditional town house in Kyoto, Japan. In our study, we have developed a lateral loading system in order to apply large shear deformation angle of 0.2 rad. Based on our tests, some new findings have been acquired as follows. (a) No pillar breaks until the horizontal restoring force is lost due to the  $P\Delta$  effect. (b) Concentration of deformation or damage in a specific story will be prevented by the existence of pillars and *toriniwa* portion. (c) While houses will not slide as one-body system, some columns with small axial force move independently. (d) Some phenomena neglected in the current seismic design in Japan have been well recognized.

*Keywords: Traditional wooden houses, Static loading test,  $P\Delta$  effect, Seismic design, Uplift*

## 1. INTRODUCTION

There are many traditional wooden town houses forming the historical townscape in Kyoto, Japan. On the other hand, there are a lot of old wooden buildings collapsed in the Hyogo-ken Nanbu, Kobe earthquake in 1995. Therefore, it is important to carry out seismic retrofit of town houses in Kyoto but their seismic performance (horizontal loading capacity and deformation capacity) are not clarified enough. Supposing a two-storied town house in Kyoto, in this research, we have conducted horizontal static loading tests of two types of plane frame which passes in the ridge direction as shown in Fig.1 (a). Then, damage progress process, restoring force characteristics, behaviour of column base, and stress transmitting mechanism are discussed based on our test results.

## 2. OUTLINE OF EXPERIMENTS

### 2.1. Specimens

In order to understand the structural properties of a two-storied town house, six specimens are used for the static loading tests as shown in Fig.1(b). Two plane frames, which pass the central pillars called *daikoku-bashira* and *shokoku-bashira* in the ridge direction, are called as Specimen-D and S, respectively. The height and width of Specimen-D or S are about 5.2m and 5.8m, respectively. There are three through columns (pillars) for each specimen. There is one mud wall in Specimen-D at the first floor and there are many mud walls in the Specimen-S. The type of joints, the dimensions and material of members are determined based on the specification used in actual traditional town houses, in Kyoto. Since the tenons of beams are inserted into the *shokoku-bashira* pillar from four directions, the cross-sectional loss of the pillar is very large. Dimensions and material of principal members are listed in Table 1. The Specimen-D and Specimen-S can be divided into the room (Specimen-DR and SR) and a narrow street with open ceiling space called *toriniwa* (Specimen-DT and ST). Pillars are directly placed on the natural stones and are not fixed at all. Therefore, the sliding or uplift of pillars is free.

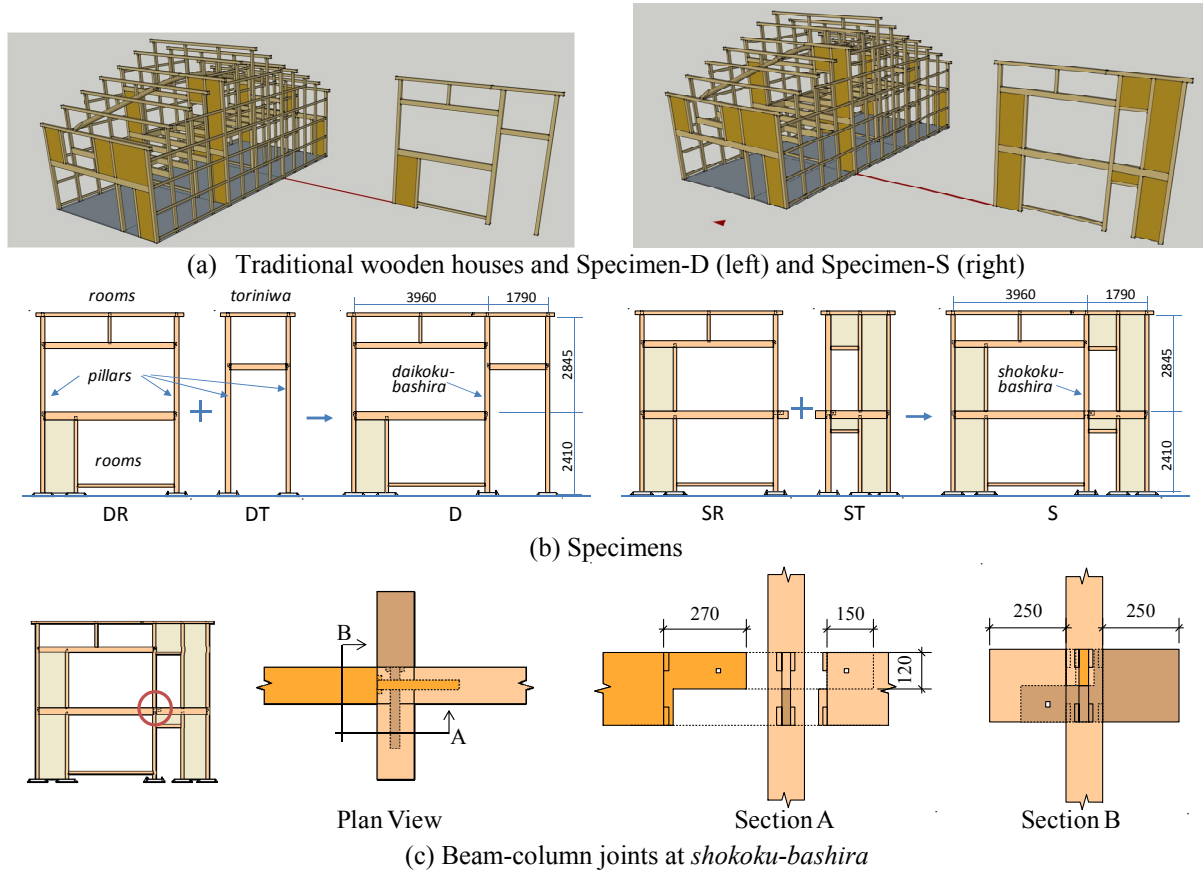


**Figure 1. Plane frame specimens in traditional town house in Kyoto**

**Table 1. Dimension and material of members**

Member	Dimension (mm)	Wood species
daikoku-bashira	150x150	Japanese cypress
shokoku-bashira	120x120	Japanese cypress
side post	120x120	Japanese cypress
stud	105x105	cedar
girder	105x240	pine
roof beam	120x180	pine
purlin	105x105	cedar
joist	90x90	cedar
roof stud	90x90	cedar

## 2.2. Loading system

Cyclic loading tests with gradually increasing displacement amplitude are conducted. The height of specimens is 5.255m. Therefore, the maximum half amplitude of displacement at the roof level is about 1.0m in order to make the maximum shear deformation angle up to 0.2 rad. To apply such a large deformation as well as vertical loads to a plane frame specimen, the following new loading system has been developed.

The loading frame consists of two plane frames. Each frame consists of two steel pillars and two horizontal steel beams and is connected each other so that their movement should be same. Pillars are supported by pin joints at the bottom, and horizontal beams are also connected to pillars by pin joints. Therefore, loading frame is unstable in the in-plane direction. In order to apply the horizontal displacement to a specimen, the specimen is connected to loading frame through load cells at roof level. In-plane horizontal displacement of the loading frame is controlled by a hydraulic jack, whose stroke is 1m, connected to the steel pillars as shown in Fig. 2(b). We perform the loading by

amplifying displacement using the principle of the lever. The loading process is shown in Fig. 2(c). The deformation angle  $R$  is the horizontal displacement of the top of the specimen divided by the height 5.255 m. The positive and minus deformation angles in this paper correspond to loading in the right and left directions, respectively.

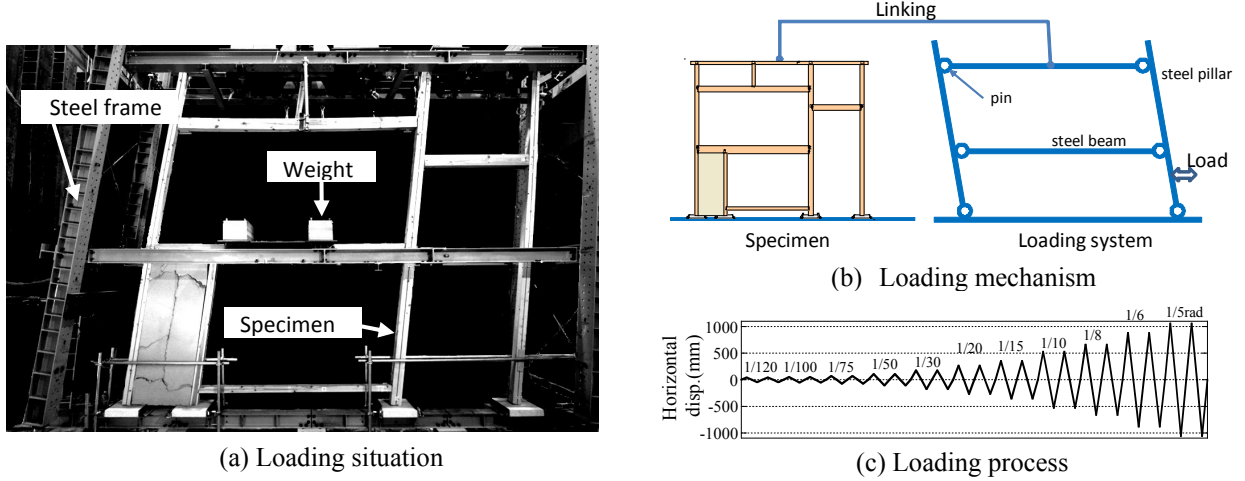
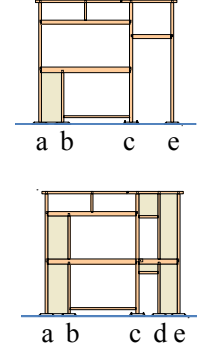


**Figure 2.** Loading system

Weights corresponding to the fixed load and movable load of a town house are set on the top and second floor level of specimens. The fixed load (weight) and movable load (the weight of specimen) is listed in Table 2. The axial force for each column is calculated and listed in Table 2. The axial forces for central through pillars are much larger than those for side through pillars. For example, the total weight of Specimen-D is about 50kN. And the axial force for the *daikoku-bashira* of Specimen-D and S, column 'c' in Table 2 is about 23kN. Therefore, half of the total weight is applied to *daikoku-bashira*.

**Table 2. Vertical load and axial force of columns**

			D	DR	DT	S	SR	ST	
Vertical load (kN)	2F	Specimen	1.6	1.1	0.8	6.6	3.0	3.9	
		Weight	30.2	16.6	15.2	30.2	16.6	15.2	
Axial force ( kN )	1F	Specimen	3.4	3.3	0.4	5.7	3.2	2.8	
		Weight	13.4	13.4	0.0	13.4	13.4	0.0	
		a	13.5	13.5	-	10.1	10.1	-	
		b	4.7	4.7	-	10.0	10.0	-	
		c	23.2	16.2	8.3	20.1	16.0	4.9	
		d	-	-	-	9.9	-	10.7	
		e	7.3	-	8.1	5.9	-	6.3	
Total (kN)			48.7	34.4	16.4	56.0	36.1	21.9	



### 3. TEST RESULTS AND DISCUSSIONS

#### 3.1. Damage progress

First, damage progress of a mud wall and frames as deformation increase is investigated. The damage to the Specimen-D and Specimen-S at deformation angle  $R=\pm 1/30$ ,  $\pm 1/15$  and  $\pm 1/8$  rad. are shown in Fig. 3. Typical damage condition of beam-column joints and uplift status of column base or mud wall are shown in Fig. 4. A mud wall in the Specimen-D starts cracking around horizontal members inside the mud wall at  $1/20$  rad. and the center of mud wall cracks in a vertical direction at  $1/15$  rad. On the other hand, mud walls in the Specimen-S cause bending cracks in both side of walls at the first floor. The cracks in the right wall develop during the rightward loading, but the cracks in the left wall develop during the leftward loading. End failure at the tenon of beams starts to occur at

the rotational angle of  $1/30$  rad. as shown in Fig. 4(a). Splitting failure occurs in the fiber direction near the cotter slot of a beam-column joint at  $1/15$  rad. as shown in Fig. 4(c). Although capital tenon and tenons at beam-column joints fractured, but no pillar breaks even if it reaches  $1/8$  rad. of deformation angle.

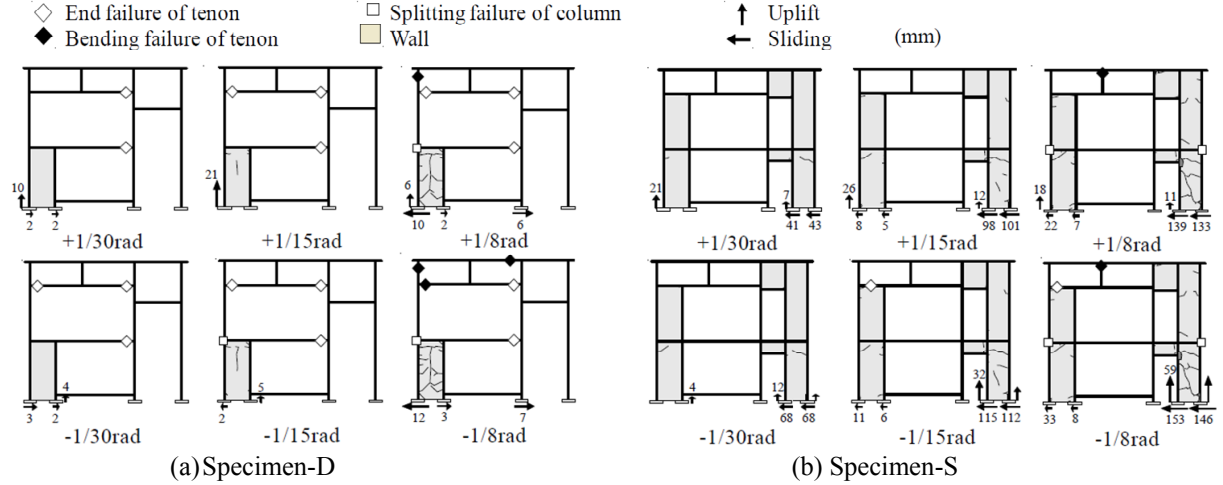


**Figure 3.** Damage process of Specimen-D and S

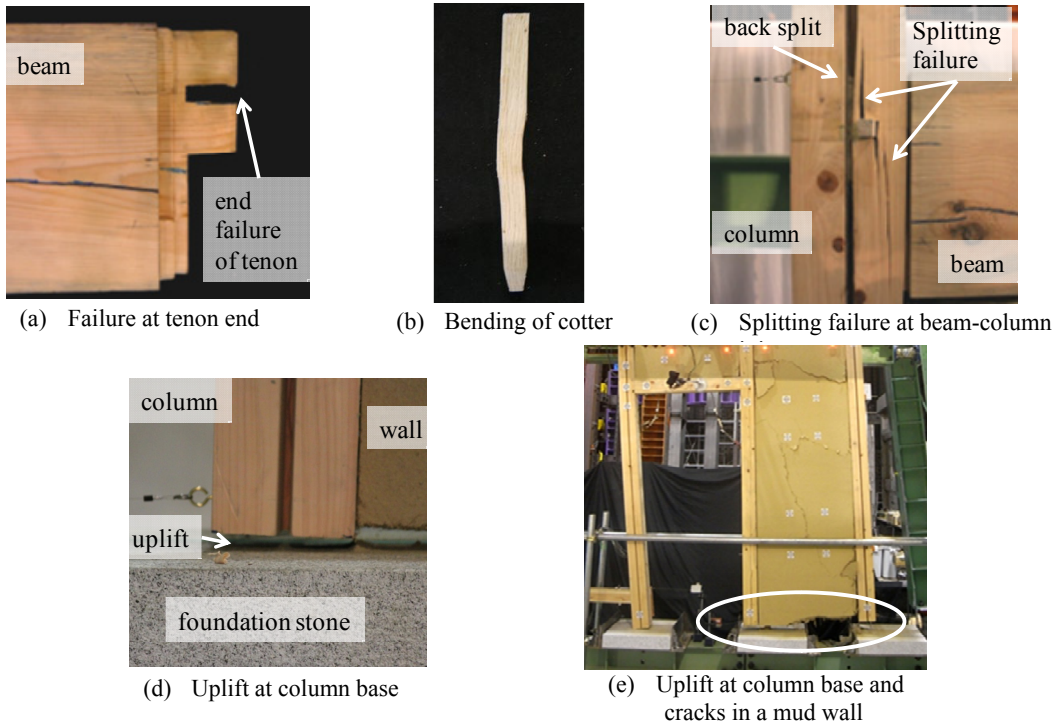


**Figure 4.** Typical damage of specimens

### 3.2. Restoring force characteristics

Figure 5 shows the restoring force characteristics for six specimens. The maximum restoring forces of the Specimen-DT in the right and left directions are about 0.5 kN. Namely, the restoring force of *toriniwa* near *daikoku-bashira* is very small. As for Specimen-D, the maximum restoring force is 4.2 kN in the right direction and 6.4 kN in the left direction. Therefore, the restoring force in the left direction is 1.5 times as large as that in the right direction. Similarly, the restoring force of Specimen-DR in the left direction is larger than that in the right direction.

As for Specimen-S, the maximum restoring force is 17.2 kN in the right direction and 12.5 kN at  $R=-0.03$  rad. in the right direction. Clearly, the restoring force characteristics of Specimen-S are asymmetrical and the maximum resisting force of Specimen-S is much larger than that of Specimen-D. The Specimen-SR, which removed the *toriniwa* from Specimen-S, shows clear reduction in the maximum resisting force in the right direction. Therefore, the *toriniwa* near *shokoku-bashira* influences notably the maximum loading capacity. Finally, the restoring force characteristics of the Specimen-ST show the rocking behaviour of the specimen. It is pointed out that difference in restoring characteristics among Specimen-S, SR and ST are dominantly affected by the difference in the axial force of *shokoku-bashira*. In addition, no damage was observed for the Specimen-ST after the loading test.

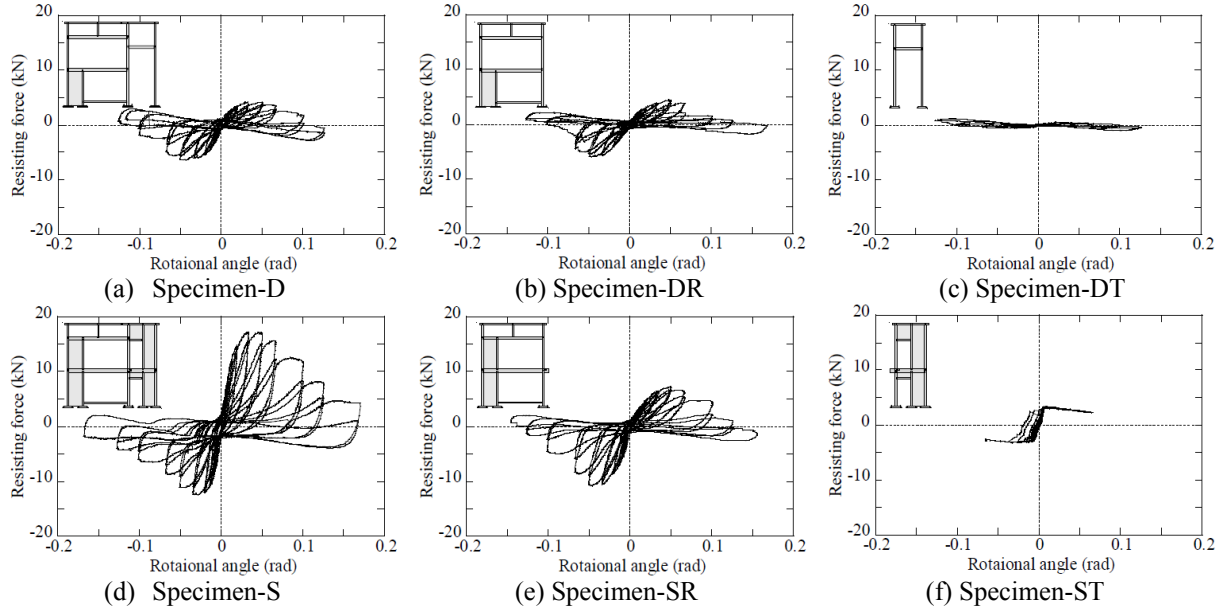


**Figure 5.** Restoring force characteristics for six specimens

Figure 6 shows the relationship between the 1<sup>st</sup> story deformation angle and 2<sup>nd</sup> story deformation angle. As for Specimen-D, the 2nd story deformation angle is 2.5 times as large as 1st story deformation angle at 1/75 rad. But the deformations of the first and second stories tend to be nearly equal as deformation angle increases. This tendency is due to the deformation equalization effects of pillars such as *daikoku-bashira* and *toriniwa*, and damage in the mud wall and beam-column joints. Namely, the *toriniwa* and pillars play a role to prevent damage concentration to the first or second story. As for Specimen-S, on the other hand, the ratio of deformations of the first to second story is dependent on loading direction. This tendency is due to the uplift of *toriniwa* in the leftward loading as described above.

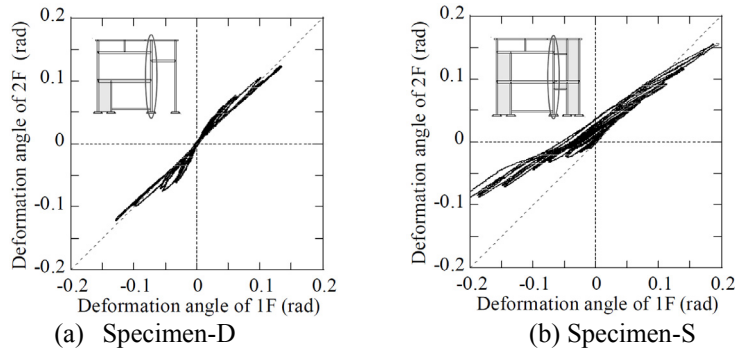


**Figure 6.** Deformation angles at the 1<sup>st</sup> and 2<sup>nd</sup> stories

### 3.3. Behaviours of column base

Uplift and sliding behaviour of columns for Specimen-D, S and ST are shown in Figs. 7 and 8. The uplift of column base occurred around a mud wall due to the tensile force induce by the rocking of the mud wall. As for Specimen-D, the uplift of side pillar, ‘a’ in Fig. 7(a), occurred under positive (rightward) loading, but the uplift of stand column, ‘b’ in Fig. 7(a), occurred under negative (leftward) loading. Column base uplift increases as shown in Fig. 7(a), as the deformation angle increases up to  $1/20$  rad. or  $1/15$  rad. After that, the uplift decreases gradually as the cracks in mud wall develop. The maximum uplift of side pillar is about 21mm and is much larger than that of stand column which is restricted to move upward by the second-floor level beam. As for Specimen-S, the uplift of stand column-‘d’ in Fig. 7(b) occurred by the loading in the right-and-left directions. The column base uplift gradually begins to decrease if the deformation angle  $R$  is  $+0.05$  rad. or more, because damage to the mud wall around the column becomes severe. However, the uplift of the column-‘d’ monotonically increases with deformation angle in the left (negative) direction due to the uplift of toriniwa shown in Fig. 4(e).

On the other hand, all the specimens do not slide as one-body system as shown in Fig. 8. This is because the ratio of the horizontal loading capacity to the total weight is much less than friction coefficient of about 0.4 between wood and stone. However, some columns with small axial force slide independently. First, the sliding of side pillar is predominant for Specimen-D after the mud wall is heavily damaged. The axial force of side pillar is not so large and the pillar moves so that the width of mud wall would spread. Next, as for Specimen-S, the column-‘d’ and ‘e’ and approaches to column-‘c’ gradually. These two columns uplift and slide in the leftward loading simultaneously to release the residual stress due to the bending cracks of the mud wall near the two columns in the rightward loading. Finally, Specimen-ST shows a rocking behavior and a pillar on either side uplift by turns as shown in Fig. 8(c). The column-‘c’ bends in the leftward loading and the distance between column-‘c’ and column-‘d’ decreases. Then, residual deformation causes when column-‘d’ lands in the unloading process as shown in Fig. 4(e). Namely, column-‘d’ and column-‘e’ moves leftward at that time. After that, the residual deformation is released just before the uplift of column-‘c’ in the rightward loading. Consequently, Specimen-ST walks to the left repeating the above process.

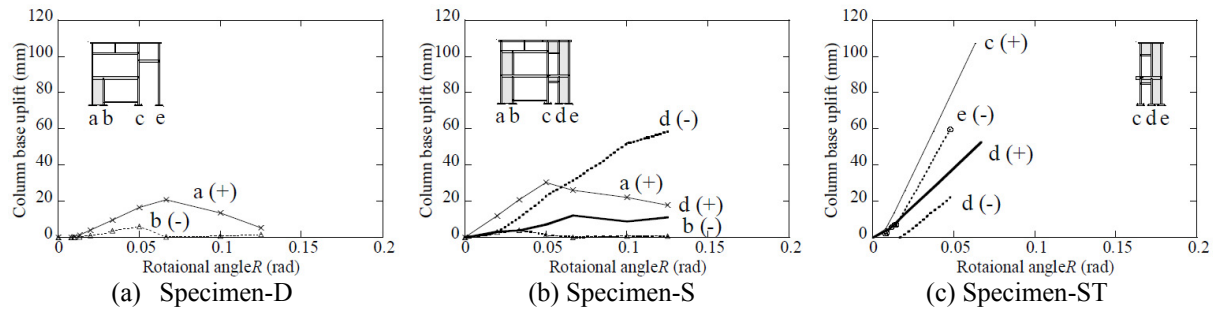


**Figure 7.** Uplift of column base

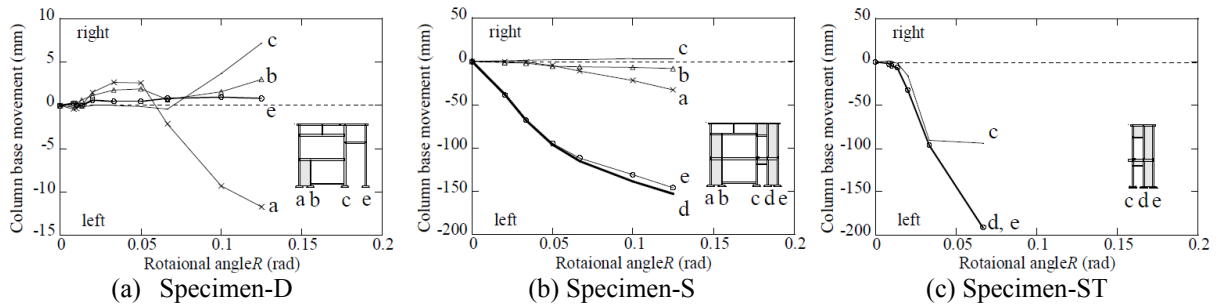


**Figure 8.** Sliding of column base

### 3.4. Stress transmitting mechanism

The shear force of columns for Specimen-D is calculated from the bending moment identified using strain gauges stuck on columns as shown in Fig. 9(a). The 1st story shear force is equal to the 2<sup>nd</sup> story shear force, because horizontal load is applied to the top of frame. Therefore, the shear force of the mud wall is calculated from those of columns as shown in Fig. 10(b). Shear force distributions and bending moment diagram for representative deformation angles are shown in Fig. 10. The maximum shear forces of mud wall in the right and left loading directions are about 7kN and 9kN, respectively, as shown in Fig. 9(b). Therefore, the maximum shear force of mud wall is larger than the maximum restoring force because there is an oppositely-directed shear force to the loading direction in the *daikoku-bashira* pillar as shown in Figs. 9 and 10. In addition, the oppositely-directed shear force decreases as the damage of mud wall become severer as shown in Figs. 9(a) and 10. Therefore, it is considered that the oppositely-directed shear force is due to the existence of the mud wall.

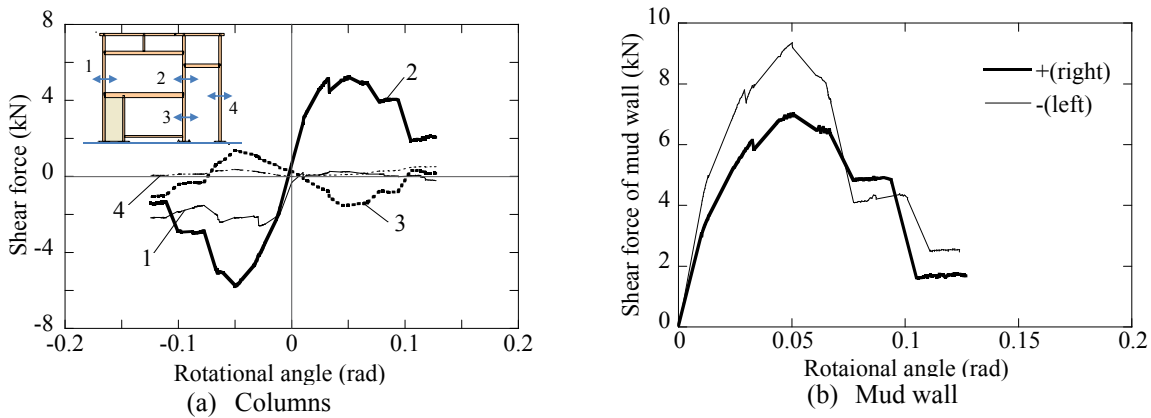


**Figure 9.** Change in shear forces

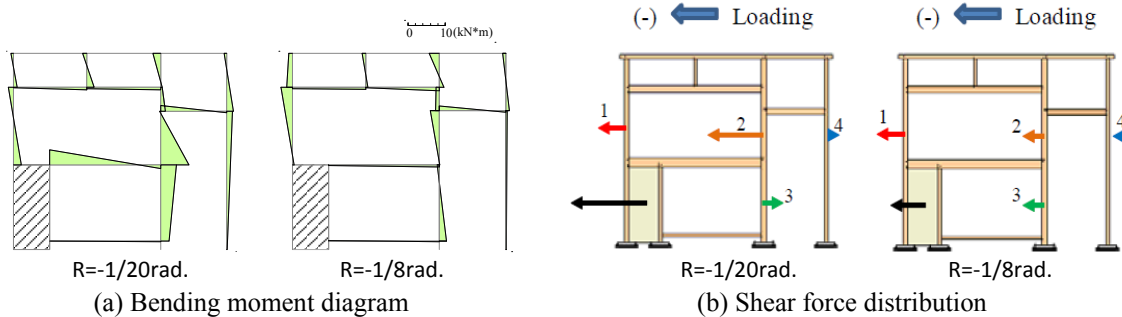


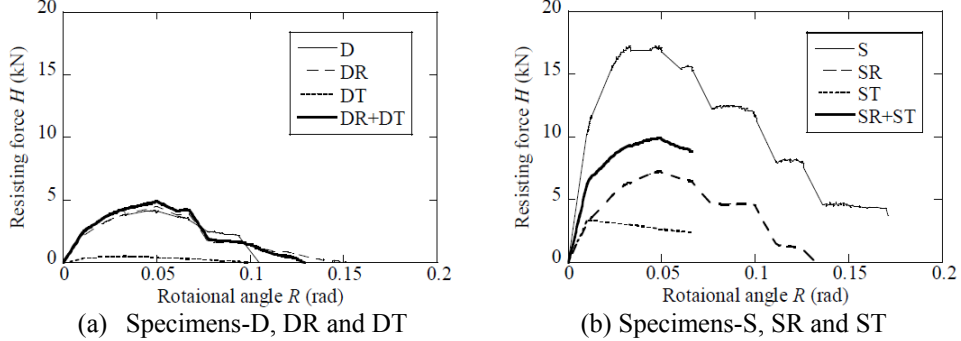
**Figure 10.** Distribution of bending moment and shear forces

### 3.5. Comparison with current design method

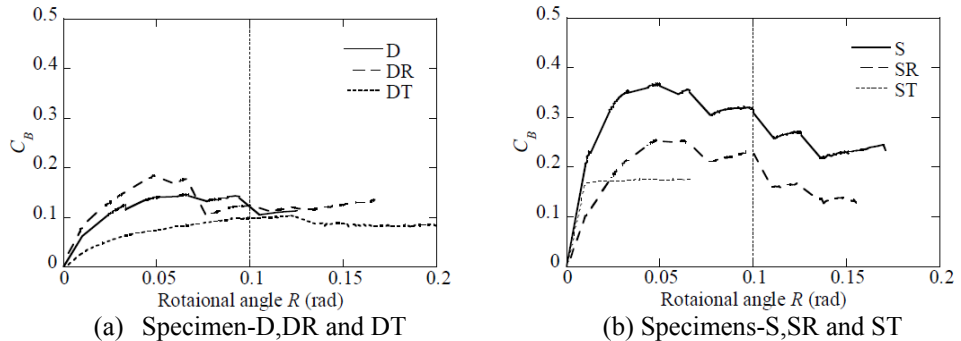
Figure 11 shows the skeleton curves of load-deformation relationship for six specimens in the rightward loading. The resisting forces are lost at 0.1 to 0.15 rad. for Specimen-D, DT and DR, but the resisting force of Specimen-S remains beyond 0.15 rad.

Figure 12 shows the base shear coefficient  $C_B$  calculated from the resisting force shown in Fig. 11 by excluding the  $P\Delta$  effects (Morii et al. (2004)) and by dividing the total weight. The restoring forces of all the specimens are held at the deformation angle  $R$  of 0.15 rad. or more. This is because stresses of the frame and mud walls are transmitted to foundation without severe damage in a through column even at the very large deformation range. Namely, the resisting forces are lost due to the  $P\Delta$  effects.

Finally, the 1<sup>st</sup> story shear forces obtained from our experimental test results and estimation by the current design method are compared in Fig. 13. The experimental result is calculated from the load-deformation relationship by excluding the  $P\Delta$  effects. Estimation by the current design method is based on the summation of skeleton curves for unit structural elements and is depicted by thin solid line with symbols in Fig. 13. Therefore, it is pointed out that the asymmetrical restoring force characteristics with respect to the loading directions are not considered in the current design (MLIT (2004)). Furthermore, the loading capacity estimated from the current design method drastically decreases due to the failure in the mud wall. However, according to the experimental results, the Specimen-D and Specimen-S hold large restoring forces even at the deformation angle of 1/10 rad as shown in Fig. 13.



**Figure 11. Resisting forces at the top of specimens**



**Figure 12. Base shear coefficients**

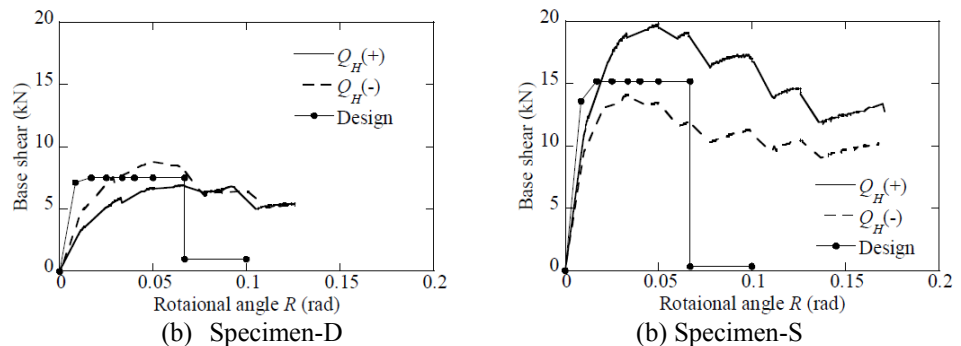


**Figure 13. Comparison of experiment and current design about base shear force**

## 4. CONCLUSIONS

We have conducted static loading tests of some plane frame of a two-storied traditional town house in Kyoto, Japan. In our study, we have developed a lateral loading system in order to apply large shear deformation angle of 0.2 rad. Based on our tests, the deformation performance and stress transferring mechanism of town houses are well understood as follows.

- (a) No pillar breaks until the horizontal restoring force is lost due to the  $P\Delta$  effect.
- (b) Concentration of deformation or damage in a specific story will be prevented by the existence of pillars and *toriniwa* portion.
- (c) Since the ratio of the horizontal loading capacity to the total weight for Specimen-S and D is less than frictional coefficient between column base and foundation stone, specimen frame does not slide as one-body system. However, some columns with small axial force move independently.
- (d) The following phenomena, which are neglected in the current seismic design method for the traditional wooden buildings in Japan, have been observed.
  - 1) Uplift of columns near a mud wall and mud wall itself
  - 2) Asymmetric restoring force characteristics
  - 3) Oppositely-directed shear force to the loading direction

## ACKNOWLEDGEMENT

This research was supported by Grants-in-Aid for Scientific Research (A) (No. 22246072), in Japan. In manufacture of the specimens, we have received great cooperation of Mr. K.Suekawa and Mr. Y.Tsuji.

## REFERENCES

- Morii, M., Miyamoto, M., Takahashi, H. and Hayashi, Y. (2010). Influence of  $P\Delta$  Effects on Deformation Capacity of Wooden Frame Structure, *Journal of Structural and Construction Engineering*, Trans. of AIJ, **650**, pp.849-857 (in Japanese).
- Ministry of Land, Infrastructure, Transport and Tourism (MLIT) (2004). Article 84 of the Enforcement Ordinance of the Building Standards Law (in Japanese).